International Journal of Non–Linear Mechanics 169 (2025) 104966

Contents lists available at ScienceDirect

International Journal of Non-Linear Mechanics

journal homepage: www.elsevier.com/locate/nlm

A general solution procedure for nonlinear single degree of freedom systems including fractional derivatives

Bengi Yıldız [a,*], Sümeyye Sınır [b], Berra Gültekin Sınır [c]

[a] Department of Mathematics, Faculty of Science, Bilecik Şeyh Edebali University, Bilecik, 11100, Türkiye
[b] General Coordination Office of Project, İzmir Katip Çelebi University, İzmir, 35620, Türkiye
[c] Department of Civil Engineering, Faculty of Engineering, Manisa Celal Bayar University, Manisa, 45140, Türkiye

ARTICLE INFO

Keywords:
Fractionally damped model
Multiple time scale method
Fractional derivative
Single-degree-of-freedom system
General solution

ABSTRACT

This paper considers oscillations of systems with a single-degree-of-freedom (SDOF) including fractional derivatives. The system is assumed to be an unforced condition. A general solution procedure that can be effectively applied to various types of fractionally damped models, where damping is defined by a fractional derivative, in engineering and physics is proposed. The nonlinearity of the mentioned models contains not only damping but can also consist of acceleration or displacement. This study proposed a new general model that includes but not limited to modified fractional versions of the well-known linear, quadratic, Coulomb and negative damped models. The method of multiple time scales is performed to obtain approximate analytical solutions. The solution, the amplitude, and the phase in the applications are plotted for various fractional derivative parameter values. In order to confirm their validity, our results for the case of the fractional derivative parameter equal to one are compared with others available in the literature.

1. Introduction

Single-degree-of-freedom (SDOF) systems are fundamental in understanding vibrations and structural dynamics. SDOF systems are extensively used across various fields, including structural engineering, mechanical vibrations [1], vibration isolation systems (energy harvesting systems) [2,3], acoustic engineering (acoustic and noise control) [4], and biomechanics (human body modeling) [5]. The equation of motion for an SDOF system typically involves a second-order differential equation, which can include forces dependent on position, velocity, or time. Examples of SDOF systems include a particle moving along an axis, a pendulum swinging in a vertical plane, or interlocking cogwheels in a machine [6]. In the literature, SDOF systems' free vibration, response to harmonic and periodic excitations, and applications have been extensively covered [7]. The physical meaning of SDOF equations relates to the system's mass, stiffness, and damping properties, which determine its dynamic behavior under various loading conditions. SDOF systems offer insights into the basic dynamic behavior that can be extended to multi-degree-of-freedom (MDOF) and continuous systems [1,5,8]. Specifically, discretizing continuous systems for numerical solutions often leads to solving systems of equations derived from SDOF models. Given their importance in understanding more complex systems, addressing SDOF equations is crucial for building a strong analytical foundation.

The main goal of employing fractional order derivatives in mathematical models rather than integer order derivatives is to better fit the real data, and overcome the restrictions of the latter. In recent years, interest in fractional calculus has increased considerably, resulting in many scholars trying to apply fractional calculus to describe their models in engineering, physics, and mechanics. (see [9–16] and references therein). Detailed explanations of the theory of fractional calculus and its applications are provided in [17–19].

Differential equations with fractional derivatives are solved using a various methods and numerical techniques when they cannot be solved analytically [20,21]. The perturbation method, an approximate analytical method, is one of the techniques used to solve the mentioned differential equations. Looking for approximations of analytical solutions to vibration problems, one of the most popular perturbation techniques is the method of multiple time scales. [6,22–24].

Damping is a force that is a function of the velocity. There are linear and nonlinear damping models in the literature. Linear damping assumes a proportional relationship between the damping force and velocity, providing a simplified but useful model for many practical applications. However, linear damping fails to capture the full range of dynamic responses in numerous real engineering systems, particularly those subjected to large displacements, high velocities, or complex material behavior. In such cases, nonlinear damping, where the damping

* Corresponding author.
E-mail addresses: bengi.yildiz@bilecik.edu.tr (B. Yıldız), sumeyye.sinir@ikcu.edu.tr (S. Sınır), gultekin.sinir@cbu.edu.tr (B.G. Sınır).

https://doi.org/10.1016/j.ijnonlinmec.2024.104966
Received 5 June 2024; Received in revised form 13 November 2024; Accepted 18 November 2024
Available online 26 November 2024

force depends on a higher order or more complicated velocity function, offers a more accurate representation. Damping has a major role in vibration isolation across single-degree-of-freedom, multi-degree-of-freedom, and continuous systems. For this reason, understanding its effects in single-degree-of-freedom systems provides a foundational approach before exploring more complex systems.

For single-degree-of-freedom dynamic systems, common damped models are linear [25], nonlinear [25–30], Coulomb [31,32], negative [1], and quadratic [33–35] damped models, etc. Along with these, the literature includes models that incorporate various combinations of these damping mechanisms [33,35], e.g., in Ref. [33], a nonlinear damping model is proposed with both quadratic and cubic damping, which is deduced from a nonlinear Rayleigh-type gradient dissipation function. In order to more precisely analyze damping effects in complicated structures or nonlinear systems, fractionally damped models are employed [11,27,36,37]. For instance, Ref. [27] by Marco Amabili derives a nonlinear damping model from a fractional viscoelastic standard solid model and shows that it can accurately reproduce the large increase in damping observed in experiments on various nonlinear vibrating structures.

The general solution technique provides several advantages, such as allowing researchers to address a wide range of issues without deriving specific solutions for each case, thereby saving time and effort in both analysis and computation. By examining the solution's form and characteristics, deeper insights into how being influenced system dynamics and responses can be achieved. These insights are crucial for developing more accurate predictive models and optimizing system performance. Given the significance of this approach, the literature includes studies on general solutions for systems involving various operators, such as linear operators [38], linear fractional operators [37], cubic operators with time derivatives [39], cubic nonlinear spatial differential operators [40], and cubic and quadratic nonlinear spatial differential operators [41].

This study brings to the literature the development of a general solution that eliminates the need to solve each lightly fractionally damped model, where damping is defined by a fractional derivative, individually By presenting a unified approach, this study enhances the efficiency and applicability of fractionally damped models in dynamic analysis. Moreover, the derived solution is not only comprehensive but also inherently adaptable to conventional damping models, ensuring consistency and compatibility with existing theoretical frameworks [1]. This approach provides a more convenient and easy tool for researchers and engineers by revealing the connection between fractional and classical models in various damping scenarios. While the general solution developed in this study offers significant advantages, it is subject to certain constraints that, although potentially viewed as limitations, also create opportunities for future research and refinement. One such restriction is omitting the quadratic stiffness term in the perturbative solution. When the approach of two terms being expanded is applied, the quadratic stiffness term vanishes due to its mathematical properties in the context of the limited expansion. As a result, it is not considered in the solution.

The most significant novelty is that this paper presents a general solution for analyzing the unforced oscillations of a nonlinear fractionally damped single-degree-of-freedom systems, offering a unified approach that eliminates the need to handle each problem independently. A general solution procedure, including the fractional derivative in the damping, has been developed for linear and nonlinear models. Thus, the novel general model is employed to find approximate solutions to linear and nonlinear problems and to demonstrate the applicability of fractionally damped models. The method of multiple time scales is used with Fourier series expansions. The general approximate analytical solutions, the general equations of amplitude and phase modulation are obtained. The suitability and effectiveness of the general solution procedure proposed in this study are validated by examining various damping mechanisms; such as fractionally linear damped, fractionally quadratic damped, fractionally Coulomb damped and fractionally negative damped models; and is also validated with cubic nonlinear fractional single-degree-of-freedom system applications. The exact solution, the amplitude, and the phase graphs are displayed according to the variation of α. It has been observed that as α increases, the damping effect also increases, except for the negative damped case when the commencing amplitude is less than the stable amplitude.

2. Equation of motion

Consider the following non-homogeneous and dimensionless model:

$$\ddot{u} + \omega_0^2 u = \varepsilon f(u, \ddot{u}, D^\alpha u) \tag{1}$$

here ε represents a dimensionless perturbation parameter, $f(u, \ddot{u}, D^\alpha u)$ is a general either linear or non-linear function of u, and D^α denotes the operator with fractional order α as the damping in the system.

The function f incorporates both cubic stiffness and nonlinear damping, which are related to the ε parameter. The multiple-time scales method, which is used for the solution method, is a perturbative solution technique. In classical perturbative solution techniques, $\varepsilon \ll 1$. If the ε value is taken as greater than 1, the results obtained by numerical solution techniques differ from the solutions obtained by using either the multiple-time scale method or another classical perturbative approach [42]. In other words, only in $\varepsilon \ll 1$, the results obtained by multiple-time scale method and numerical methods agree and give similar values. The physical equivalent of ε being less than 1 in the mathematical model is the weakly nonlinear stiffness and lightly damping. Some studies consider strongly nonlinear (i.e., ε is greater than one) [43]. In these studies, solutions were obtained using a non-classical perturbative expansion technique. However, since the classical perturbative solution approach is used in this study, ε must be less than 1.

Although there exist several definitions of the fractional-order derivative based on different backgrounds, the most widely employed in engineering fields of these are Caputo and Riemann–Liouville definitions. The dynamic response of a nonlinear viscoelastic oscillator has been demonstrated to produce mathematical models of the nonlinear viscoelastic phenomenon that are completely equivalent, subject to certain minimal restrictions, according to the Riemann–Liouville and Caputo definitions [44,45]. In this paper, Riemann–Liouville's definition introduced in the case $0 < \alpha < 1$ is (see formula (5.6) in [46])

$$D^\alpha f(t) = \frac{1}{\Gamma(1-\alpha)} \frac{d}{dt} \int_{-\infty}^{t} \frac{f(s)}{(t-s)^\alpha} ds, \tag{2}$$

where Γ represents the Gamma function.

From the definition in (2), one obtains the fractional derivative of the exponential function and cosine function as, respectively:

$$D^\alpha e^{\mathrm{i}\omega t} = (\mathrm{i}\omega)^\alpha e^{\mathrm{i}\omega t} + \frac{\sin \pi\alpha}{\pi} \int_0^\infty \frac{u^\alpha e^{-ut}}{u + \mathrm{i}\omega} du \tag{3}$$

and

$$D^\alpha \cos \omega t = \omega^\alpha \cos\left(\omega t + \frac{\pi}{2}\alpha\right) + \frac{\sin \pi\alpha}{\pi} \int_0^\infty \frac{u^{1+\alpha} e^{-ut}}{u^2 + \omega^2} du. \tag{4}$$

If the exact formulas (3) and (4) are used for the fractional differentiation of the exponential function and cosine function, then the integral entering in Eqs. (3) and (4) determine that part of the solution which describes the drift of the position of oscillator's equilibrium [47]. However, these integrals decay rapidly with time, and in many cases (see [14,47,48]), they can be neglected as compared with the first term in Eqs. (3) and (4). Reference to Eqs. (3) and (4) show that if α differs slightly from the unit when the fractional parameter α value is small, and for rather large ω frequencies, then the integrals in the right-hand side of Eqs. (3) and (4) can be neglected. This case is realized for single-degree-of freedom systems, as an example, in the vicinity of natural frequencies of systems [49]. What allows one to use the fractional derivative of the exponential function as

$$D^{\alpha} e^{i\omega t} = (i\omega)^{\alpha} e^{i\omega t}, \tag{5}$$

and the fractional derivative of the cosine function as

$$D^{\alpha} \cos \omega t = \omega^{\alpha} \cos\left(\omega t + \frac{\pi}{2}\alpha\right). \tag{6}$$

The Riemann–Liouville fractional derivative definition is used in mathematical model (1) to describe the damping features. Because since the second terms of (3) and (4) will influence the solution only beginning from the second-order approximation in the solution method, the Caputo and the Riemann–Liouville fractional derivative will be completely equivalent to the solution (24) within the limits of the zero and first-order approximations. Therefore, under these conditions, it does not matter which definition is used [44].

3. Solution method

The method of multiple time scales is directly applied to Eq. (1). An approximate solution function is assumed in the following expansion:

$$u(t;\varepsilon) = u_0(T_0, T_1, \dots) + \varepsilon u_1(T_0, T_1, \dots) + \cdots, \tag{7}$$

where the T_n, $i = 1, 2, \dots$ are defined by

$$T_0 = t, \quad T_1 = \varepsilon t, \dots$$

Here, each variable represents a different time scale: T_0 is the fastest, T_1 is slower, and so on. Time derivatives are expressed in terms of fast and slow time scales [49,50]:

$$\frac{d}{dt} = D_0 + \varepsilon D_1 + \dots, \tag{8}$$

$$\frac{d^2}{dt^2} = D_0{}^2 + 2\varepsilon D_0 D_1 + \dots, \tag{9}$$

$$\left(\frac{d}{dt}\right)^{\alpha} = D^{\alpha} + \varepsilon \alpha D^{\alpha-1} D_1 + \cdots \tag{10}$$

where D_n represents $\frac{\partial}{\partial T_n}$.

Substituting u from (7) and time derivatives from (8)–(10) into Eq. (1) and determining each of the coefficients of ε^0 and ε, one has following equations.

$$O(1):\ D_0{}^2 u_0 + \omega_0^2 u_0 = 0 \tag{11}$$

$$O(\varepsilon):\ D_0{}^2 u_1 + \omega_0^2 u_1 = -2 D_0 D_1 u_0 + f(u_0, D_0{}^2 u_0, D^{\alpha} u_0) \tag{12}$$

The complex solution form at ε^0-order is

$$u_0(T_0, T_1) = A(T_1) e^{i\omega_0 T_0} + \bar{A}(T_1) e^{-i\omega_0 T_0}, \tag{13}$$

where i denotes complex number $\sqrt{-1}$, and $\bar{A}$ is the complex conjugate function of A.

A is determined by eliminating the secular terms. Considering Eq. (5) and substituting for u_0 into Eq. (12), one gets

$$\begin{aligned} D_0{}^2 u_1 + \omega_0^2 u_1 = {} & -2i\omega_0 D_1 A e^{i\omega_0 T_0} + 2i\omega_0 D_1 \bar{A} e^{-i\omega_0 T_0} \\ & + f\Big(A e^{i\omega_0 T_0} + \bar{A} e^{-i\omega_0 T_0}, -\omega_0^2 A e^{i\omega_0 T_0} - \omega_0^2 \bar{A} e^{-i\omega_0 T_0}, \\ & A (i\omega_0)^{\alpha} e^{i\omega_0 T_0} + \bar{A}(-i\omega_0)^{\alpha} e^{-i\omega_0 T_0}\Big) \end{aligned} \tag{14}$$

In order to perform a valid expansion, secular terms are eliminated from u_0. To this end $f(u_0, D_0{}^2 u_0, D^{\alpha} u_0)$ is expanded in a Fourier series

$$f = \sum_{n=-\infty}^{\infty} f_n(A, \bar{A}) e^{in\omega_0 T_0} \tag{15}$$

where

$$f_n(A, \bar{A}) = \frac{\omega_0}{2\pi} \int_0^{2\pi/\omega_0} f e^{-in\omega_0 T_0} dT_0. \tag{16}$$

After eliminating secular terms from (14), the following condition is obtained

$$-2i\omega_0 D_1 A + f_n(A, \bar{A}) = 0. \tag{17}$$

Then,

$$2i D_1 A = \frac{1}{2\pi} \int_0^{2\pi/\omega_0} f e^{-i\omega_0 T_0} dT_0. \tag{18}$$

is obtained. To solve (18), it is suitable to exhibit $A(T_1)$ in the following polar form:

$$A(T_1) = \frac{1}{2} a(T_1) e^{i\beta(T_1)} \tag{19}$$

Thereby (13) is rewritten as

$$u_0 = a(T_1)\cos\phi, \qquad \phi = \omega_0 T_0 + \beta(T_1). \tag{20}$$

Inserting (6) and (19) into (18) yields

$$i(a' + ia\beta') = \frac{1}{2\pi\omega_0} \int_0^{2\pi} f(a\cos\phi, -a\omega_0^2 \cos\phi, \omega_0{}^{\alpha} a \cos\left(\phi + \frac{\pi\alpha}{2}\right)) e^{-i\phi} d\phi. \tag{21}$$

For simplicity, here (′) denotes derivative with respect to T_1, and a and β denotes $a(T_1)$ and $\beta(T_1)$, subsequently. Dividing real and imaginary parts, respectively

$$a' = -\frac{1}{2\pi\omega_0} \int_0^{2\pi} \sin\phi f(a\cos\phi, -a\omega_0^2\cos\phi, \omega_0{}^{\alpha} a\cos\left(\phi + \frac{\pi\alpha}{2}\right)) d\phi \tag{22}$$

$$\beta' = -\frac{1}{2\pi\omega_0 a} \int_0^{2\pi} \cos\phi f(a\cos\phi, -a\omega_0^2\cos\phi, \omega_0{}^{\alpha} a\cos\left(\phi + \frac{\pi\alpha}{2}\right)) d\phi \tag{23}$$

are calculated. Hence the approximate solution of (1) is

$$u = a(T_1)\cos(\omega_0 T_0 + \beta(T_1)) + O(\varepsilon), \tag{24}$$

where a and β can be calculated by solving relations (22) and (23) subsequently.

4. Applications

In this section, fractionally linear damped, fractionally quadratic damped, fractionally Coulomb damped, fractionally negative damped models, nonlinear problems involving such models and nonlinear fractional equations are considered applications. These problems are solved using the proposed general solution procedure.

4.1. Fractionally linear damped single-degree-of-freedom system

The linear damped model has been widely studied by researchers, and in Refs. [25,29], fractional or non-fractional versions of the linear damped model are examined. Now, consider the fractionally linear damped model as,

$$\ddot{u} + \omega_0^2 u = -2\varepsilon\mu D^{\alpha} u. \tag{25}$$

Therefore corresponding f is

$$f(u_0, D_0{}^2 u_0, D^{\alpha} u_0) = -2\mu D^{\alpha} u_0 = -2\mu\omega_0{}^{\alpha} a \cos\left(\phi + \frac{\pi\alpha}{2}\right),$$

then (22) and (23) become

$$\begin{aligned} a' &= -\frac{1}{2\pi\omega_0} \int_0^{2\pi} \sin\phi \left(-2\mu\omega_0{}^{\alpha} a\cos\left(\phi + \frac{\pi\alpha}{2}\right)\right) d\phi \\ &= -\mu\omega_0^{\alpha-1} a \sin\left(\frac{\pi\alpha}{2}\right) \end{aligned} \tag{26}$$

$$\begin{aligned} \beta' &= -\frac{1}{2\pi\omega_0 a} \int_0^{2\pi} \cos\phi \left(-2\mu\omega_0{}^{\alpha} a\cos\left(\phi + \frac{\pi\alpha}{2}\right)\right) d\phi \\ &= \mu\omega_0^{\alpha-1} \cos\left(\frac{\pi\alpha}{2}\right) \end{aligned} \tag{27}$$

Solving (26) and (27) gives

$$a = a_0 e^{-\varepsilon\mu\omega_0^{\alpha-1} \sin\left(\frac{\pi\alpha}{2}\right) t}, \qquad \beta = \varepsilon\mu\omega_0^{\alpha-1}\cos\left(\frac{\pi\alpha}{2}\right) t + \beta_0, \tag{28}$$

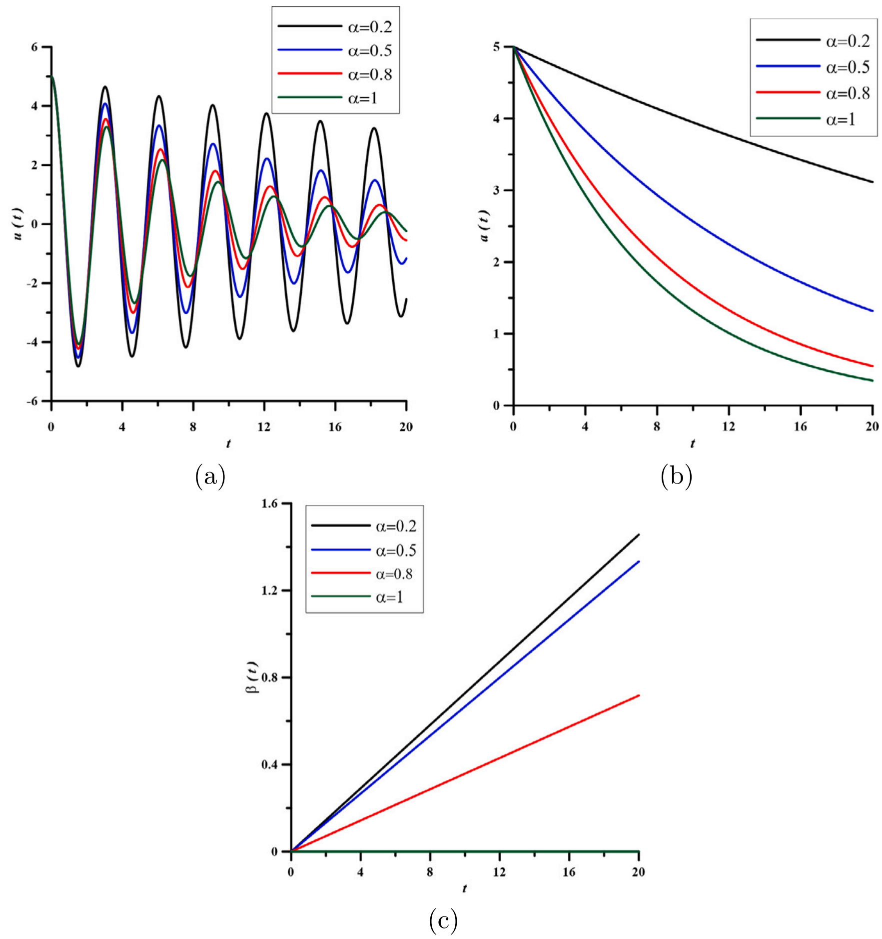

Fig. 1. (a) The approximate solution $u(t)$, (b) the amplitude $a(t)$ and (c) the phase $\beta(t)$ of fractionally linear damped single-degree-of-freedom system with for $\varepsilon = 1/3$, $a_0 = 5$, $\mu = 0.4$, $\omega_0 = 2$, $\beta_0 = 0$.

where a_0 and β_0 are constants. Therefore, (24) becomes

$$u = a_0 e^{-\varepsilon\mu\omega_0^{\alpha-1}\sin\left(\frac{\pi\alpha}{2}\right)t}\cos\left(\left(\omega_0 + \varepsilon\mu\omega_0^{\alpha-1}\cos\left(\frac{\pi\alpha}{2}\right)\right)t + \beta_0\right) + O(\varepsilon) \tag{29}$$

Fig. 1 shows the effects of linear fractional viscous damping on displacement, amplitude, and phase. In the time history graph shown in Fig. 1.(a), the amplitude varies with time. This variation is given in Fig. 1.(b). It is seen that the phase values given in Fig. 1.(c) change with time for different fractional derivative values. In Fig. 1.(c), the change of β over time is linear.

As the parameter α approaches 1, the behavior of the fractional-order derivative aligns more closely with that of the conventional derivative. This convergence emerges the damping effect, which becomes more dominant. Namely, as the fractional derivative parameter increases, the damping of the amplitude also increases. At low values of the fractional derivative parameter, the reduction in amplitude follows a nearly linear trend. However, as the fractional derivative parameter value increases, the amplitude decay becomes nonlinear.

In contrast, when α approaches 0, the fractional-order derivative itself vanishes, causing its coefficient to act similarly to a stiffness coefficient. Thereby, the stiffness effect becomes more dominant. This effect is also observed in Fig. 1.(c).

In essence, the fractional derivative parameter influences amplitude, thereby influencing the system's natural frequency. In other words, in the fractionally damped case, the natural frequency varies with the damping and the stiffness.

In Eqs. (28) and (29) if one takes $\alpha = 1$, i.e., not fractional versions of (28) and (29), the corresponding equations become solutions of linear damped systems (see Eqs. (3.3.29) and (3.3.30) in [1]). Additionally, for $\alpha = 1$, the phase β is unchanged with time. That means, for $\alpha = 1$, variation of frequency is not affected by viscosity. For $\alpha = 1$, the results obtained are observed to be consistent with those of [1].

4.1.1. Fractionally linear damped duffing equation

Consider the well-known fractionally linear damped nonlinear Duffing equation, i.e.

$$\ddot{u} + {\omega_0}^2 u = -2\varepsilon\mu D^{\alpha} u - \varepsilon u^3. \tag{30}$$

Considering model is specific version of the model introduced in Refs. [29,51]. Then,

$$f(u_0, {D_0}^2 u_0, D^{\alpha} u_0) = -2\mu D^{\alpha} u_0 - {u_0}^3 = -2\mu{\omega_0}^{\alpha} a\cos\left(\phi + \frac{\pi\alpha}{2}\right) - a^3\cos^3\phi,$$

and corresponding Eqs. (22) and (23) become

$$\begin{aligned} a' &= -\frac{1}{2\pi\omega_0}\int_0^{2\pi}\sin\phi\left(-2\mu{\omega_0}^{\alpha} a\cos\left(\phi + \frac{\pi\alpha}{2}\right) - a^3\cos^3\phi\right)d\phi \\ &= -\mu\omega_0^{\alpha-1}\sin\left(\frac{\pi\alpha}{2}\right)a \end{aligned} \tag{31}$$

$$\begin{aligned} \beta' &= -\frac{1}{2\pi\omega_0 a}\int_0^{2\pi}\cos\phi\left(-2\mu{\omega_0}^{\alpha} a\cos\left(\phi + \frac{\pi\alpha}{2}\right) - a^3\cos^3\phi\right)d\phi \\ &= \mu\omega_0^{\alpha-1}\cos\left(\frac{\pi\alpha}{2}\right) + \frac{3a^2}{8\omega_0} \end{aligned} \tag{32}$$

Solving (31) and (32) gives

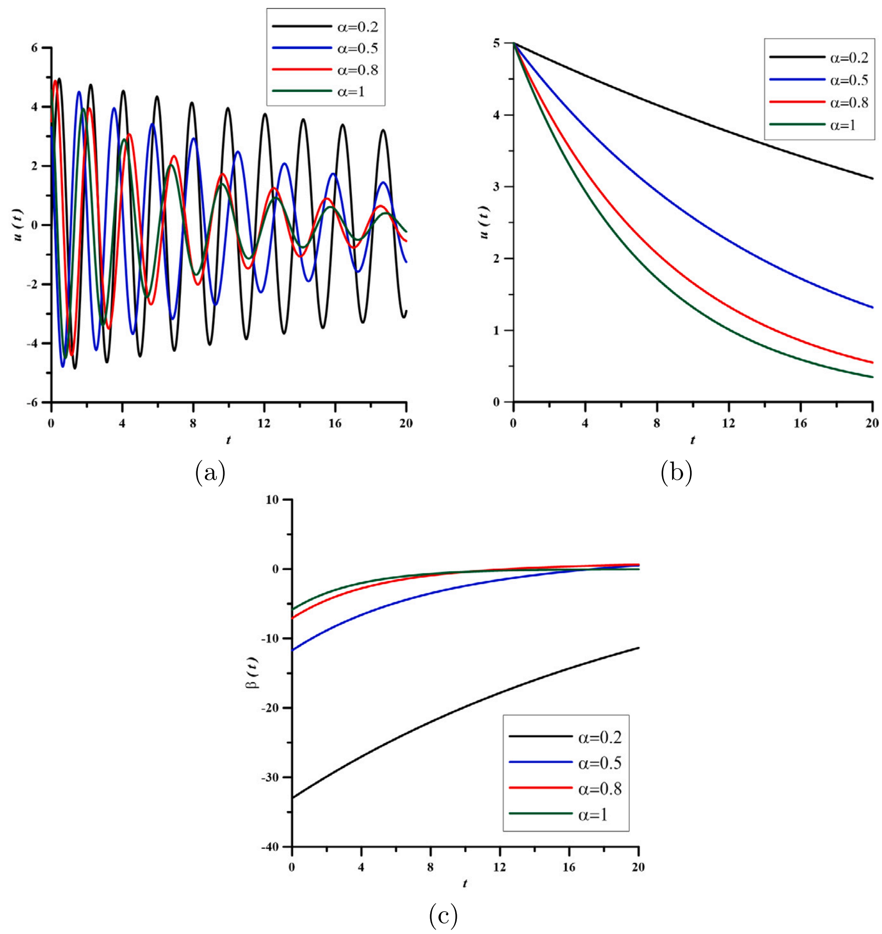

Fig. 2. (a) The approximate solution $u(t)$, (b) the amplitude $a(t)$ and (c) the phase $\beta(t)$ of fractionally linear damped Duffing equation with for $\varepsilon = 1/3$, $a_0 = 5$, $\mu = 0.4$, $\omega_0 = 2$, $\beta_0 = 0$.

$$a = a_0 e^{-\varepsilon\mu\omega_0^{\alpha-1}\sin\left(\frac{\pi\alpha}{2}\right)t}, \tag{33}$$

$$\beta = -\frac{3}{16}\frac{a_0^2 e^{-2\varepsilon t\mu\omega_0^{\alpha-1}\sin\left(\frac{\pi\alpha}{2}\right)}}{\mu\omega_0^{\alpha}\sin\left(\frac{\pi\alpha}{2}\right)} + \mu\omega_0^{\alpha-1}\cos\left(\frac{\pi\alpha}{2}\right)\varepsilon t + \beta_0 \tag{34}$$

where a_0 and β_0 are constants. Therefore, (24) becomes

$$u = a_0 e^{-\varepsilon\mu\omega_0^{\alpha-1}\sin\left(\frac{\pi\alpha}{2}\right)t}\cos\left(\begin{array}{c}\omega_0 t - \frac{3}{16}\frac{a_0^2 e^{-2\varepsilon t\mu\omega_0^{\alpha-1}\sin\left(\frac{\pi\alpha}{2}\right)}}{\mu\omega_0^{\alpha}\sin\left(\frac{\pi\alpha}{2}\right)} \\ +\mu\omega_0^{\alpha-1}\cos\left(\frac{\pi\alpha}{2}\right)\varepsilon t + \beta_0\end{array}\right) + O(\varepsilon) \tag{35}$$

Fig. 2 shows the application of the linear fractional derivative to the Duffing equation, which is a nonlinear model. It can be seen in Fig. 2.(b) that the presence of the fractional derivative reduces the vibration amplitude over time, exhibiting a trend similar to that observed in the linear model case. However, the fractional derivative's effect on the phase of the nonlinear model differs from its effect in the linear model, as seen in Fig. 2.(c). The phase remains negative for all fractional derivative values. As the fractional derivative value increases, the change in phase decreases and approaches zero after a certain time step.

In summary, as the parameter α approaches 1, the damping effect of the fractional derivative becomes increasingly pronounced, while as α nears 0, the term's contribution shifts towards a stiffness-dominant behavior. This evolution is further illustrated in Fig. 2.(c), where the stiffness effect declines nonlinearly over time before reaching a stable value.

If $\alpha = 1$ in Eqs. (33), (34), and (35), the corresponding equations become solutions of the wellknown Duffing equation (see [52]).

4.1.2. Fractionally linear viscous damped single-degree-of-freedom system with nonlinear inertia

Let consider the modified model of the equation from [52] as follows,

$$\ddot{u} + \omega_0^2 u = -\varepsilon u^2\ddot{u} - 2\varepsilon\mu(D^{\alpha}u) \tag{36}$$

Here, the damping is linear. Thus,

$$\begin{aligned} f(u_0, {D_0}^2 u_0, D^{\alpha}u_0) &= -u_0^2 {D_0}^2 u_0 - 2\mu(D^{\alpha}u_0) \\ &= \omega_0^2 a^3\cos^3\phi - 2\mu\omega_0^{\alpha} a\cos\left(\phi + \frac{\pi\alpha}{2}\right) \end{aligned} \tag{37}$$

Inserting (36) into (22) and (23), the following equations are obtained

$$\begin{aligned} a' &= -\frac{1}{2\pi\omega_0}\int_0^{2\pi}\sin\phi\left(\omega_0^2 a^3\cos^3\phi - 2\mu\omega_0^{\alpha} a\cos\left(\phi + \frac{\pi\alpha}{2}\right)\right)d\phi \\ &= -{\omega_0}^{\alpha-1}\mu a\sin\left(\frac{\pi\alpha}{2}\right) \end{aligned} \tag{38}$$

$$\begin{aligned} \beta' &= -\frac{1}{2\pi\omega_0 a}\int_0^{2\pi}\cos\phi\left({\omega_0}^2 a^3\cos^3\phi - 2\mu{\omega_0}^{\alpha} a\cos\left(\phi + \frac{\pi\alpha}{2}\right)\right)d\phi \\ &= -\frac{3}{8}a^2\omega_0 + \omega_0^{\alpha-1}\mu\cos\left(\frac{\pi\alpha}{2}\right). \end{aligned} \tag{39}$$

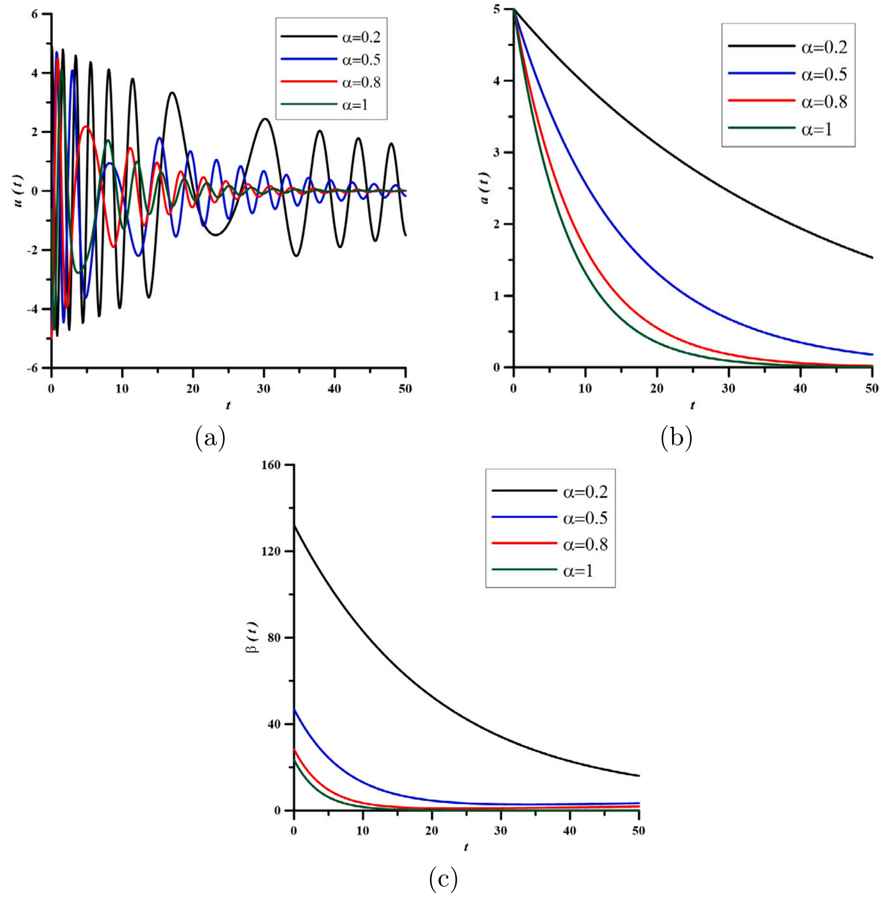

Fig. 3. (a) The solution function $u(t)$, (b) the amplitude $a(t)$, and (c) the phase $\beta(t)$ of a fractionally linear damped single-degree-of-freedom system with nonlinear inertia term and for $\varepsilon = 1/3$, $\mu = 0.4$, $a_0 = 5$, $\omega_0 = 2$, $\beta_0 = 0$.

Integrating (38) and (39) yields,

$$a = a_0 e^{-\varepsilon\mu\omega_0^{\alpha-1}\sin\left(\frac{\pi\alpha}{2}\right)t} \tag{40}$$

and

$$\beta = \frac{3}{16}\frac{a_0^2 e^{-2\varepsilon t\mu\omega_0^{\alpha-1}\sin\left(\frac{\pi\alpha}{2}\right)}}{\mu\omega_0^{\alpha}\sin\left(\frac{\pi\alpha}{2}\right)} + \mu\omega_0^{\alpha-1}\cos\left(\frac{\pi\alpha}{2}\right)\varepsilon t + \beta_0 \tag{41}$$

where a_0 and β_0 are constants. Consequently, (24) is obtained with a and β, which are given by (40) and (41), respectively. Therefore, (24) becomes

$$u = a_0 e^{-\varepsilon\mu\omega_0^{\alpha-1}\sin\left(\frac{\pi\alpha}{2}\right)t}\cos\left(\begin{array}{c}\omega_0 t + \dfrac{3}{16}\dfrac{a_0^2 e^{-2\varepsilon t\mu\omega_0^{\alpha-1}\sin\left(\frac{\pi\alpha}{2}\right)}}{\mu\omega_0^{\alpha}\sin\left(\frac{\pi\alpha}{2}\right)} \\ +\mu\omega_0^{\alpha-1}\cos\left(\frac{\pi\alpha}{2}\right)\varepsilon t + \beta_0\end{array}\right) + O(\varepsilon) \tag{42}$$

Fig. 3 shows the results of applying the linear fractional damping to the model containing nonlinear inertia. The damping effect is seen in Fig. 3.(a). In this model, the fractional linear viscous damping affects the change of amplitude, slightly different from previous models (Fig. 3.(b)). The decrease in amplitude over time follows a curvilinear trajectory for all values of the fractional derivative. Similarly, the variation of phase difference over time is slightly different from previous models (Fig. 3.(c)). Here, phase variation over time is also curvilinear and remains positive across all fractional derivative values, eventually approaching zero. Namely, the stiffness effect becomes zero as α approaches 1.

As seen in the first two applications for fractional linear damping, one observes that obtained solutions coincide with solutions in the literature, when $\alpha = 1$. Thus, for this modified equation, when $\alpha = 1$, received results are valid for non-fractional case.

4.2. Fractionally quadratic damped single-degree-of-freedom system

The equation of a fractionally quadratic damped single-degree-of-freedom system is in the following form:

$$\ddot{u} + \omega_0^2 u = -\varepsilon D^{\alpha}u|D^{\alpha}u| \tag{43}$$

Hence,

$$\begin{aligned} f(u_0, {D_0}^2u_0, D^{\alpha}u_0) &= -D^{\alpha}u_0|D^{\alpha}u_0| = -Sgn(D^{\alpha}u_0)(D^{\alpha}u_0)^2 \\ &= -{\omega_0}^{2\alpha}a^2\cos\left(\phi + \frac{\pi\alpha}{2}\right)\left|\cos\left(\phi + \frac{\pi\alpha}{2}\right)\right|, \end{aligned} \tag{44}$$

where

$$Sgn(D^{\alpha}u_0) = \begin{cases} 1, & D^{\alpha}u_0 > 0, \\ 0, & D^{\alpha}u_0 = 0, \\ -1, & D^{\alpha}u_0 < 0. \end{cases} \tag{45}$$

Then (22) and (23) become

$$a' = -\frac{1}{2\pi\omega_0}\int_0^{2\pi}\sin\phi\left(-{\omega_0}^{2\alpha}a^2\cos\left(\phi + \frac{\pi\alpha}{2}\right)\left|\cos\left(\phi + \frac{\pi\alpha}{2}\right)\right|\right)d\phi \tag{46}$$

$$\beta' = -\frac{1}{2\pi\omega_0 a}\int_0^{2\pi}\cos\phi\left(-{\omega_0}^{2\alpha}a^2\cos\left(\phi + \frac{\pi\alpha}{2}\right)\left|\cos\left(\phi + \frac{\pi\alpha}{2}\right)\right|\right)d\phi \tag{47}$$

Then, (46) and (47) expressions are

$$a' = -\frac{4\omega_0^{2\alpha-1}\sin\left(\frac{\pi\alpha}{2}\right)a^2}{3\pi}, \tag{48}$$

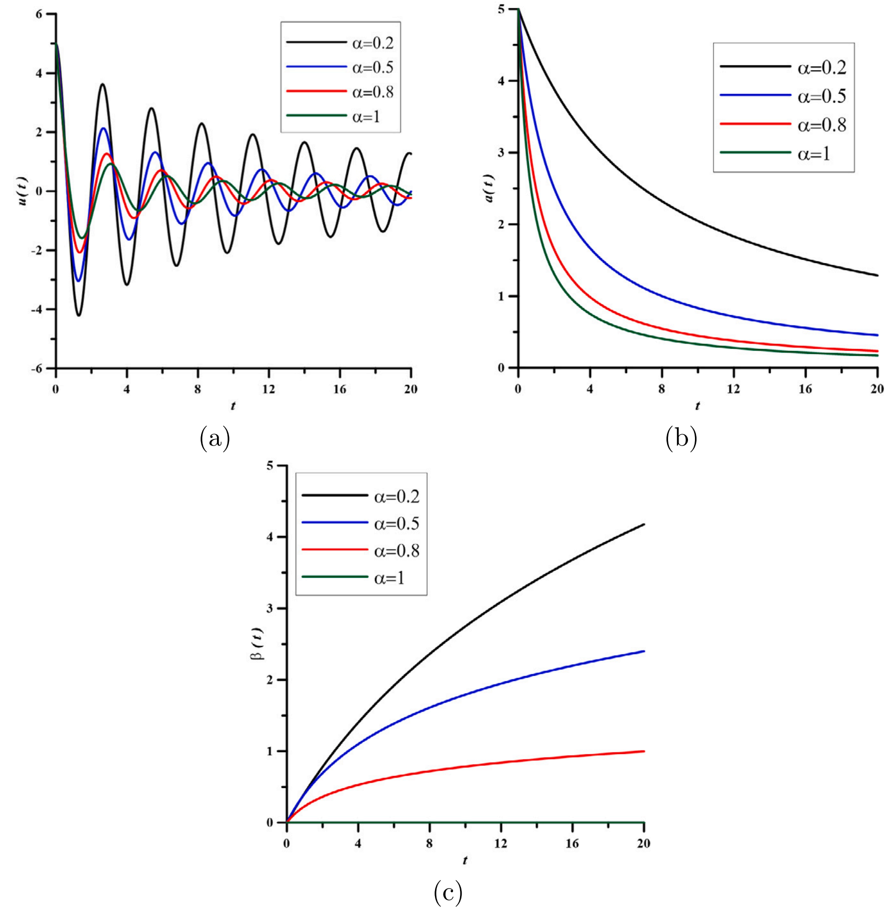

Fig. 4. (a) The solution function $u(t)$, (b) the amplitude $a(t)$, and (c) the phase $\beta(t)$ of a fractionally quadratic damped single-degree-of-freedom system for $\varepsilon = 1/3$, $a_0 = 5$, $\omega_0 = 2$, $\beta_0 = 0$.

$$\beta' = \frac{4\omega_0^{2\alpha-1}\cos\left(\frac{\pi\alpha}{2}\right)a}{3\pi}. \tag{49}$$

The amplitude is obtained as follows by solving the ordinary differential equation (48),

$$a = \frac{a_0}{1 + \dfrac{4\varepsilon a_0\omega_0^{2\alpha-1}\sin\left(\frac{\pi\alpha}{2}\right)}{3\pi}t} \tag{50}$$

Additionally, after solving the differential equation obtained by replacing (50) into (49) β can be obtained as follows:

$$\beta = \cot\left(\frac{\pi\alpha}{2}\right)\ln\left(\frac{4\omega_0^{2\alpha-1}\sin\left(\frac{\pi\alpha}{2}\right)\varepsilon a_0}{3\pi}t + 1\right) + \beta_0 \tag{51}$$

where a_0 and β_0 are constants. Consequently, (24) is obtained with a and β, which are given by (50) and (51), respectively. Therefore, (24) becomes

$$u = \frac{a_0\cos\left(\omega_0 t + \cot\left(\frac{\pi\alpha}{2}\right)\ln\left(\frac{4a_0\omega_0^{2\alpha-1}\sin\left(\frac{\pi\alpha}{2}\right)\varepsilon t}{3\pi} + 1\right) + \beta_0\right)}{1 + \frac{4a_0\omega_0^{2\alpha-1}\sin\left(\frac{\pi\alpha}{2}\right)\varepsilon t}{3\pi}} + O(\varepsilon) \tag{52}$$

The effects of the quadratic fractional damping on the time–history graphic (Fig. 4.(a)), the amplitude of the vibrations (Fig. 4.(b)), and phase difference (Fig. 4.(c)) are shown. The variations of vibration amplitude of the quadratic fractional damping are similar to the linear fractional damping in contrast to the phase diagram. Phase values increase curvilinearly with time. The slope of the phase curve lines decreases as the fractional derivative value increases. When α equals one, the phase difference vanishes, indicating an absence of the stiffness effect. In other words, the classical quadratic damping does not affect the natural frequency, still the fractional damping has an effect on the natural frequency depending on the fractional derivative value.

Suppose one takes $\alpha = 1$ in Eqs. (50), (51), and (52), the corresponding equations become solutions of quadratic damped systems (see [1]).

4.3. Fractionally Coulomb damped single-degree-of-freedom system

The equation of motion of fractionally Coulomb damped model is in the following form:

$$\ddot{u} + \omega_0^2 u = \begin{cases} -\varepsilon\mu \text{ when } D^\alpha u > 0 \\ \varepsilon\mu \text{ when } D^\alpha u < 0 \end{cases} \tag{53}$$

Substituting for the corresponding f, which is

$$f(u_0, {D_0}^2 u_0, D^\alpha u_0) = \begin{cases} -\mu \text{ when } D^\alpha u_0 > 0 \\ \mu \text{ when } D^\alpha u_0 < 0, \end{cases} \tag{54}$$

into (22) and (23), and similar to the fractionally quadratic damped case when splitting the integration, one has

$$a' = -\frac{2\mu\sin\left(\frac{\pi\alpha}{2}\right)}{\pi\omega_0}, \tag{55}$$

$$\beta' = \frac{2\mu\cos\left(\frac{\pi\alpha}{2}\right)}{\pi\omega_0 a} \tag{56}$$

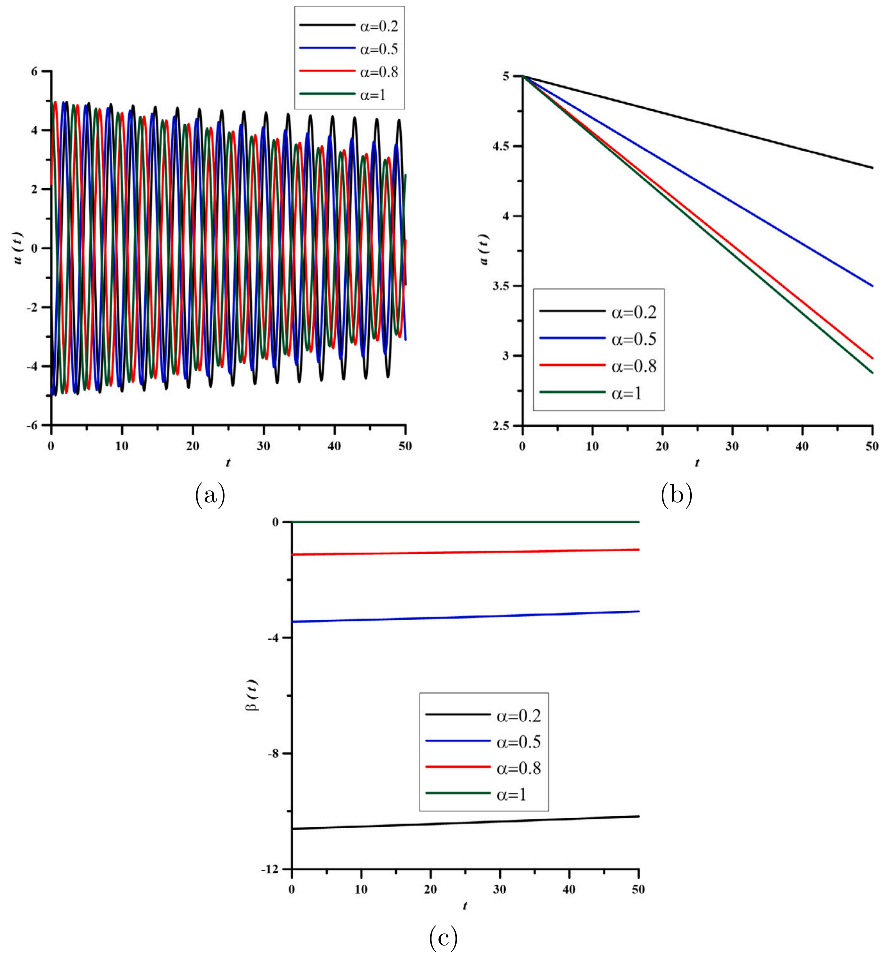

Fig. 5. (a) The solution function $u(t)$, (b) the amplitude $a(t)$ and (c) the phase $\beta(t)$ of fractionally Coulomb damped single-degree-of-freedom system for $\varepsilon = 1/3$, $a_0 = 5$, $\mu = 0.4$, $\omega_0 = 2$, $\beta_0 = 0$.

The amplitude is obtained as follows by solving the ordinary differential equation (55),

$$a = -\frac{2\mu \sin\left(\frac{\pi\alpha}{2}\right)}{\pi\omega_0}\varepsilon t + a_0 \tag{57}$$

Hence, the amplitude decreases linearly with time. Additionally, after solving obtained differential equation by replacing (57) into (56), β can be calculated as follows:

$$\beta = -\cot\left(\frac{\pi\alpha}{2}\right)\ln\left(-2\mu\sin\left(\frac{\pi\alpha}{2}\right)\varepsilon t + \pi\omega_0 a_0\right) + \beta_0 \tag{58}$$

where a_0 and β_0 are constants. Consequently, (24) is obtained with a and β, which are given by (57) and (58), respectively. Therefore, (24) becomes

$$u = \left(\frac{-2\mu\sin\left(\frac{\pi\alpha}{2}\right)\varepsilon t}{\pi\omega_0} + a_0\right) \times \cos\left(\omega_0 t - \ln\left(-2\mu\sin\left(\frac{\pi\alpha}{2}\right)\varepsilon t + \pi\omega_0 a_0\right)^{\cot\left(\frac{\pi\alpha}{2}\right)} + \beta_0\right) + O(\varepsilon) \tag{59}$$

The effect of the fractional Coulomb damping on the dynamic behavior of the single-degree-of-freedom system is seen in Fig. 5. The effect of the fractional derivative is slightly different in the Coulomb damped model than in the viscous linear and quadratic damped models. As the value of the fractional derivative approaches 1, the rate of decrease in vibration amplitude also increases, so it is observed that the damping effect increases. The decrease in vibration amplitude changes linearly with time for all fractional derivative values. However, the phase difference remains constant, with distinct values depending on the fractional derivative. Similar to the quadratic damping, for $\alpha = 1$, the phase difference in the Coulomb damping is zero, signifying the absence of a stiffness effect.

When $\alpha = 1$ in Eqs. (57), (58), and (59), the corresponding equations become solutions of Coulomb damped systems (see [1]).

4.4. Fractionally negative damped single-degree-of-freedom system

Consider Rayleigh's equation, which is a cubic nonlinear equation governing the oscillations of systems having a fractionally negative damped single-degree-of-freedom.

$$\ddot{u} + {\omega_0}^2 u = \varepsilon(D^\alpha(u) - (D^\alpha(u))^3). \tag{60}$$

Therefore for this case, corresponding f in (1) is

$$\begin{aligned} f(u_0, {D_0}^2 u_0, D^\alpha u_0) &= (D^\alpha(u_0) - (D^\alpha(u_0))^3) \\ &= \omega_0^\alpha a\cos\left(\phi + \frac{\pi\alpha}{2}\right) - \omega_0^{3\alpha} a^3 \cos^3\left(\phi + \frac{\pi\alpha}{2}\right) \end{aligned} \tag{61}$$

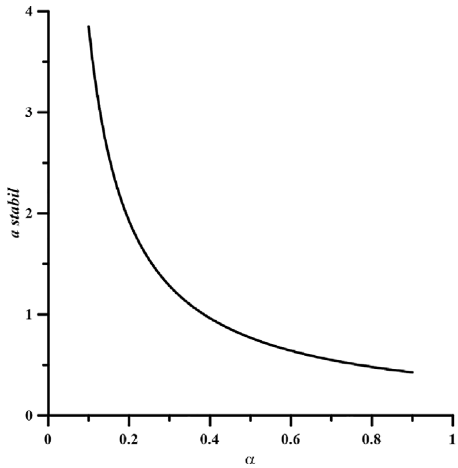

Fig. 6. Variation of a_s according to α.

Substituting (61) into (22) and (23),

$$a' = -\frac{1}{2\pi\omega_0}\int_0^{2\pi} \sin\phi\left(\omega_0^{\alpha} a\cos\left(\phi+\frac{\pi\alpha}{2}\right) - \omega_0^{3\alpha}a^3\cos^3\left(\phi+\frac{\pi\alpha}{2}\right)\right)d\phi$$
$$= \frac{1}{2}{\omega_0}^{\alpha-1}a\sin\left(\frac{\pi\alpha}{2}\right) - \frac{3}{8}{\omega_0}^{3\alpha-1}a^3\sin\left(\frac{\pi\alpha}{2}\right) \tag{62}$$

$$\beta' = -\frac{1}{2\pi\omega_0 a}\int_0^{2\pi} \cos\phi\left(\omega_0^{\alpha} a\cos\left(\phi+\frac{\pi\alpha}{2}\right) - \omega_0^{3\alpha}a^3\cos^3\left(\phi+\frac{\pi\alpha}{2}\right)\right)d\phi$$
$$= -\frac{1}{2}{\omega_0}^{\alpha-1}\cos\left(\frac{\pi\alpha}{2}\right) + \frac{3}{8}{\omega_0}^{3\alpha-1}a^2\cos\left(\frac{\pi\alpha}{2}\right) \tag{63}$$

are obtained. Integrating (62) and (63) yields,

$$a = \pm\frac{a_0}{\sqrt{\left(1-\frac{3}{4}{\omega_0}^{2\alpha}{a_0}^2\right)e^{-\omega_0^{\alpha-1}\sin\left(\frac{\pi\alpha}{2}\right)\varepsilon t} + \frac{3}{4}{\omega_0}^{2\alpha}{a_0}^2}} \tag{64}$$

$$\beta = \frac{-\omega_0^{\alpha-1}\varepsilon t\sin(\pi\alpha)}{4\sin\left(\frac{\pi\alpha}{2}\right)} + \frac{1}{2}\cot\left(\frac{\pi\alpha}{2}\right)\ln\left(\frac{4e^{-\omega_0^{\alpha-1}\sin\left(\frac{\pi\alpha}{2}\right)\varepsilon t}a_0 + 3{\omega_0}^{2\alpha}}{e^{-\omega_0^{\alpha-1}\sin\left(\frac{\pi\alpha}{2}\right)\varepsilon t}}\right) + 4\beta_0 \tag{65}$$

where a_0 and β_0 are constants. Consequently, (24) is obtained with a and β, which are given by (64) and (65), respectively. Therefore, (24) becomes

$$u = \pm\frac{a_0\cos\left(\begin{array}{c}\omega_0 t - \frac{\omega_0^{\alpha-1}\varepsilon t\sin(\pi\alpha)}{4\sin\left(\frac{\pi\alpha}{2}\right)} + 4\beta_0 + \\ \frac{1}{2}\cot\left(\frac{\pi\alpha}{2}\right)\ln\left(\frac{4e^{-\omega_0^{\alpha-1}\sin\left(\frac{\pi\alpha}{2}\right)\varepsilon t}a_0+3{\omega_0}^{2\alpha}}{e^{-\omega_0^{\alpha-1}\sin\left(\frac{\pi\alpha}{2}\right)\varepsilon t}}\right)\end{array}\right)}{\sqrt{\left(1-\frac{3}{4}{\omega_0}^{2\alpha}{a_0}^2\right)e^{-\omega_0^{\alpha-1}\sin\left(\frac{\pi\alpha}{2}\right)\varepsilon t} + \frac{3}{4}{\omega_0}^{2\alpha}{a_0}^2}} + O(\varepsilon) \tag{66}$$

Eq. (64) demonstrates that the oscillation's amplitude converges to $a_s = \frac{2}{\sqrt{3\omega_0^{\alpha}}}$, independently of the initial amplitude's value, provided that it does not equal zero. Eq. (62) demonstrates that when a is greater than a_s, the derivative a' is negative, which indicates that a tends to decrease. Conversely, when a is less than a_s, the derivative a' is positive, which indicates that a tends to increase. The value of a being equal to a_s represents a steady amplitude.

In Fig. 6, the a_s varies depending on α has been demonstrated in the fractionally negative damped case. As the α increases, Fig. 6 illustrates that a_s decreases curvilinearly.

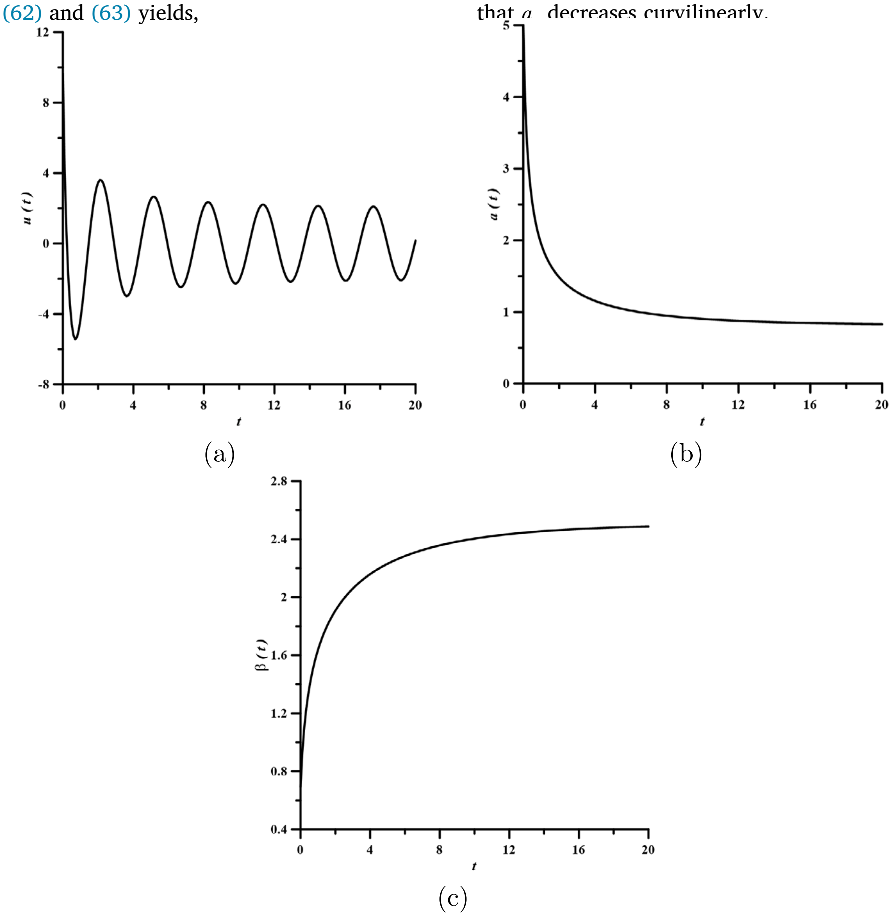

Fig. 7. (a) The solution function $u(t)$, (b) the amplitude $a(t)$, and (c) the phase $\beta(t)$ of fractionally negative damped single-degree-of-freedom system with where $a_0 > a_s$ for $\varepsilon = 1/3$, $a_0 = 5$, $\omega_0 = 2$, $\beta_0 = 0$, $\alpha = 0.5$, $a_s = 0.7698003590$.

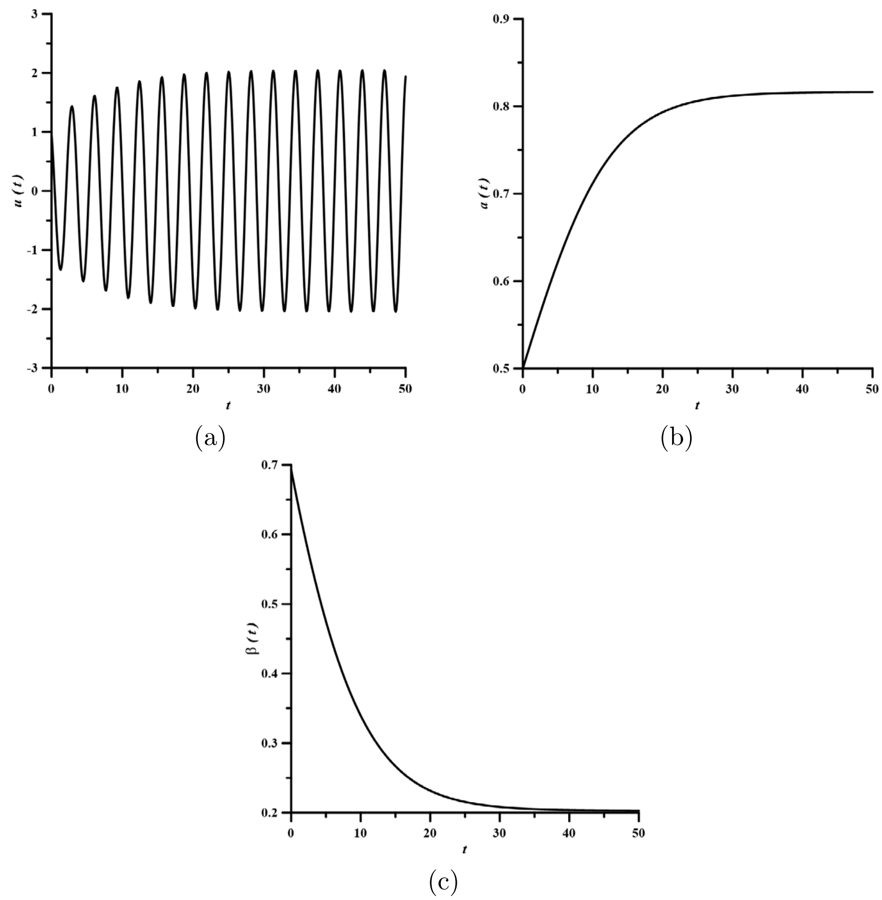

Fig. 8. (a) The solution function $u(t)$, (b) the amplitude $a(t)$ and (c) the phase $\beta(t)$ of fractionally negative damped single-degree-of-freedom system with where $a_0 < a_s$ for $\varepsilon = 1/3$, $a_0 = 0.5$, $\omega_0 = 2$, $\beta_0 = 0$, $\alpha = 0.5$, $a_s = 0.7698003590$.

In Figs. 7 and 8, the comparison of the numerical findings of (60) and the asymptotic results (64) is given for $a_0 > a_s$ and $a_0 < a_s$, subsequently. In Fig. 7, from an initial positive damping, the amplitude decays until the steady amplitude value. However, In Fig. 8, the initial damping is negative, and the amplitude rises progressively until it reaches a stable value.

If $\alpha = 1$ in Eqs. (64), (65), and (66), the corresponding equations become solutions of negative damped systems (see [1]). In 4.4.1, a special case of negative damped model, graphs of $\alpha = 1$ condition are given.

4.4.1. Fractional Van der Pol equation

Consider the fractional Van der Pol's equation, i.e.

$$\ddot{u} + {\omega_0}^2 u = \varepsilon(1 - u^2) D^{\alpha} u. \tag{67}$$

The fractional nonlinear damping introduced by this model is proportional to $u^2 D^{\alpha} u$, which is consistent with the expressions presented in similar models in Refs. [25,28,36]. Additionally, model (67) is a special case of the model in the Ref. [53]. Hence,

$$\begin{aligned} f(u_0, {D_0}^2 u_0, D^{\alpha} u_0) &= (1 - {u_0}^2) D^{\alpha} u_0 \\ &= a\omega_0^{\alpha} \cos\left(\phi + \frac{\pi\alpha}{2}\right) - a^3 \omega_0^{\alpha} \cos^2\phi \cos\left(\phi + \frac{\pi\alpha}{2}\right), \end{aligned} \tag{68}$$

and corresponding a' and β' equations are

$$\begin{aligned} a' &= -\frac{1}{2\pi\omega_0} \int_0^{2\pi} \sin\phi \\ &\quad \times \left(a\omega_0^{\alpha} \cos\left(\phi + \frac{\pi\alpha}{2}\right) - a^3 \omega_0^{\alpha} \cos^2\phi \cos\left(\phi + \frac{\pi\alpha}{2}\right) \right) d\phi \\ &= \frac{1}{2}\omega_0^{\alpha-1} \sin\left(\frac{\pi\alpha}{2}\right) a - \frac{1}{8}\omega_0^{\alpha-1} \sin\left(\frac{\pi\alpha}{2}\right) a^3 \end{aligned} \tag{69}$$

$$\begin{aligned} \beta' &= -\frac{1}{2\pi\omega_0 a} \int_0^{2\pi} \cos\phi \\ &\quad \times \left(a\omega_0^{\alpha} \cos\left(\phi + \frac{\pi\alpha}{2}\right) - a^3 \omega_0^{\alpha} \cos^2\phi \cos\left(\phi + \frac{\pi\alpha}{2}\right) \right) d\phi \\ &= -\frac{1}{2}\omega_0^{\alpha-1} \cos\left(\frac{\pi\alpha}{2}\right) + \frac{3}{8}\omega_0^{\alpha-1} \cos\left(\frac{\pi\alpha}{2}\right) a^2 \end{aligned} \tag{70}$$

Solving (69) and (70) gives

$$a = \pm \frac{a_0}{\sqrt{\left(1 - \frac{1}{4}a_0^2\right) e^{-\varepsilon\mu\omega_0^{\alpha-1} \sin\left(\frac{\pi\alpha}{2}\right) t} + \frac{1}{4}a_0^2}} \tag{71}$$

and

$$\beta = \frac{-\omega_0^{\alpha-1} \varepsilon t \sin(\pi\alpha)}{4\sin\left(\frac{\pi\alpha}{2}\right)} + \beta_0 + \frac{3}{2}\cot\left(\frac{\pi\alpha}{2}\right) \ln\left(\frac{e^{-\omega_0^{\alpha-1} \sin\left(\frac{\pi\alpha}{2}\right)\varepsilon t}(a_0^2 - 4) - a_0^2}{e^{-\omega_0^{\alpha-1} \sin\left(\frac{\pi\alpha}{2}\right)\varepsilon t}} \right) \tag{72}$$

where a_0 and β_0 are constants. Therefore, (24) becomes

$$u = \pm \frac{a_0 \cos\left(\begin{array}{c} \omega_0 t + \dfrac{-\omega_0^{\alpha-1} \varepsilon t \sin(\pi\alpha)}{4\sin\left(\frac{\pi\alpha}{2}\right)} + \beta_0 \\ + \dfrac{3}{2}\cot\left(\frac{\pi\alpha}{2}\right) \ln\left(\dfrac{e^{-\omega_0^{\alpha-1} \sin\left(\frac{\pi\alpha}{2}\right)\varepsilon t}(a_0^2 - 4) - a_0^2}{e^{-\omega_0^{\alpha-1} \sin\left(\frac{\pi\alpha}{2}\right)\varepsilon t}} \right) \end{array} \right)}{\sqrt{\left(1 - \frac{1}{4}a_0^2\right) e^{-\varepsilon\mu\omega_0^{\alpha-1} \sin\left(\frac{\pi\alpha}{2}\right) t} + \frac{1}{4}a_0^2}} + O(\varepsilon) \tag{73}$$

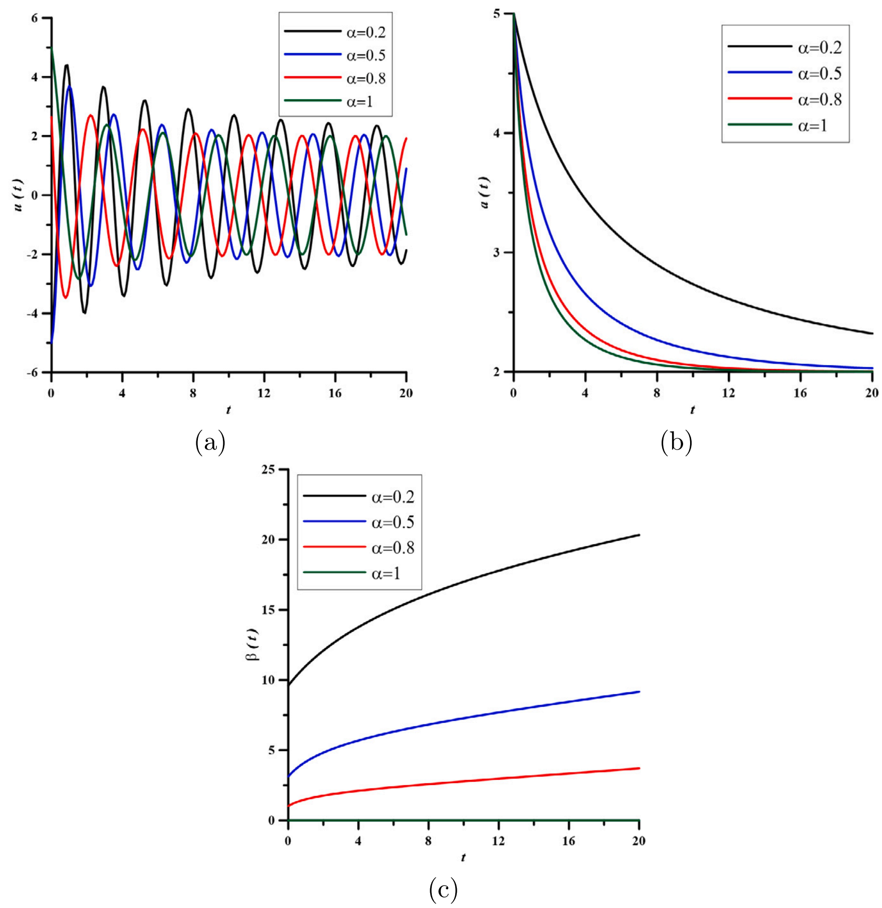

Fig. 9. (a) The solution function $u(t)$, (b) the amplitude $a(t)$ and (c) the phase $\beta(t)$ of fractional Van der Pol equation for $\varepsilon = 1/3$, $a_0 = 5$, $\omega_0 = 2$, $\beta_0 = 0$, $a_s = 2$.

The fractional Van der Pol equation is a special case of the system with negative damping, well known in the literature. The stable amplitude a_s value of the fractional Van der Pol equation has been calculated as equal to 2.

In Figs. 9 and 10, the compared diagrams of approximate solutions of (67) and the asymptotic results (71) are established for $a_0 > a_s = 2$ and $a_0 < a_s = 2$, subsequently.

In Fig. 9, from an initial positive damping, the amplitude decays until the steady amplitude value. As α increases, the vibration amplitude decreases curvilinearly faster until the steady amplitude value. However, in Fig. 10, the initial damping is negative, and the amplitude rises until the steady amplitude value. Both in Figs. 9 and 10, it is observed that the influence of fractional parameters on system stiffness and damping. As α approaches 1, the damping effect increases; meanwhile, the stiffness effect goes to zero.

4.5. The fractional cubic nonlinear single-degree-of-freedom systems

This section examines a single-degree-of-freedom models that can arise due to the discretization of viscoelastic continuum models.

4.5.1. The application to example

Consider the modified equation from [52] as follows,

$$\ddot{u} + {\omega_0}^2 u + 2\varepsilon\mu u^2 D^\alpha u + \varepsilon u^3 = 0. \tag{74}$$

Additionally, the fractional nonlinear damping introduced by this model is proportional to $u^2 D^\alpha u$ [25,28,36]. Then,

$$f(u_0, {D_0}^2 u_0, D^\alpha u_0) = -2\mu u_0^2 D^\alpha u_0 - u_0^3$$
$$= -2\mu a^3 {\omega_0}^\alpha \cos^2\phi \cos\left(\phi + \frac{\pi\alpha}{2}\right) - a^3\cos^3\phi, \tag{75}$$

Inserting (74) into (22) and (23), the following equations are obtained

$$a' = -\frac{1}{2\pi\omega_0}\int_0^{2\pi} \sin\phi\left(-2\mu a^3\cos^2\phi\,\omega_0^\alpha\cos\left(\phi+\frac{\pi\alpha}{2}\right) - a^3\cos^3\phi\right)d\phi$$
$$= -\frac{\mu a^3 {\omega_0}^{\alpha-1}}{4}\sin\left(\frac{\pi\alpha}{2}\right) \tag{76}$$

$$\beta' = -\frac{1}{2\pi\omega_0 a}\int_0^{2\pi} \cos\phi\left(-2\mu a^3\cos^2\phi\,\omega_0^\alpha\cos\left(\phi+\frac{\pi\alpha}{2}\right) - a^3\cos^3\phi\right)d\phi$$
$$= \frac{3\mu {\omega_0}^{\alpha-1} a^2}{4}\cos\left(\frac{\pi\alpha}{2}\right) + \frac{3a^2}{8\omega_0}. \tag{77}$$

Integrating (76) and (77) yields,

$$a = \pm\frac{2}{\sqrt{2\mu{\omega_0}^{\alpha-1}\sin\left(\frac{\pi\alpha}{2}\right)\varepsilon t + 4a_0}} \tag{78}$$

and

$$\beta = \frac{3}{2\mu}\cot\left(\frac{\pi\alpha}{2}\right)\ln\left(4\varepsilon t{\omega_0}^{\alpha+1}\sin\left(\frac{\pi\alpha}{2}\right) + 8a_0\omega_0^2\right)^{\frac{3}{\mu{\omega_0}^\alpha}+1} + \beta_0 \tag{79}$$

where a_0 and β_0 are constants. Consequently, (24) is obtained with a and β, which are given by (78) and (79), respectively. Therefore, (24) becomes

$$u = \pm\frac{2\cos\left(\omega t + \frac{3}{2\mu}\cot\left(\frac{\pi\alpha}{2}\right)\ln\left(4\varepsilon t{\omega_0}^{\alpha+1}\sin\left(\frac{\pi\alpha}{2}\right) + 8a_0\omega_0^2\right)^{\frac{3}{\mu{\omega_0}^\alpha}+1} + \beta_0\right)}{\sqrt{2\mu{\omega_0}^{\alpha-1}\sin\left(\frac{\pi\alpha}{2}\right)\varepsilon t + 4a_0}}$$
$$+ O(\varepsilon) \tag{80}$$

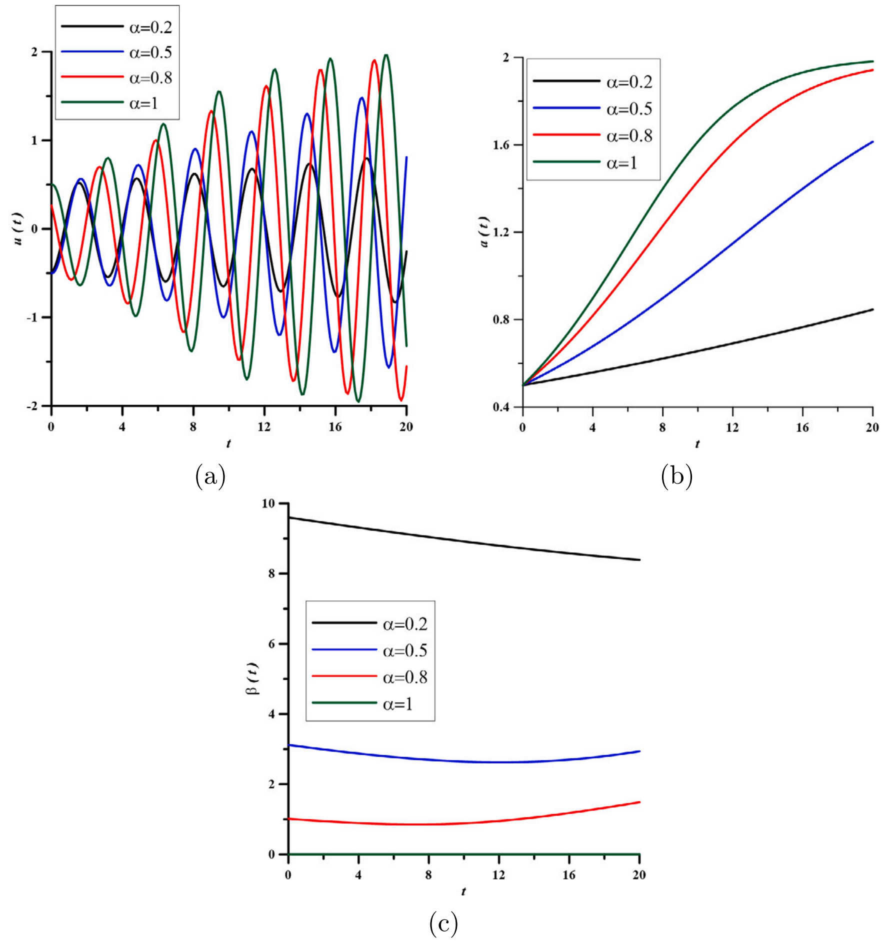

Fig. 10. (a) the solution function $u(t)$, (b) the amplitude $a(t)$ and (c) the phase $\beta(t)$ of fractional Van der Pol equation for $\varepsilon = 1/3$, $a_0 = 0.5$, $\omega_0 = 2$, $\beta_0 = 0$, $a_s = 2$.

In Fig. 11, the exact solution of (74), the variation of the amplitude and phase according to α are plotted. As α approaches 1, the damping effect becomes more pronounced, so the rate of amplitude change increases. Whereas as α approaches 0, the stiffness effect dominates. Also, the rate of phase change remains nearly constant. Like in previous applications, non-fractional graphs of the equation are given in Fig. 11, for comparison.

Models similar to Eq. (74) are obtained by discretizating Kelvin–Voigt-type viscoelastic continuous media such as beams, strips, etc., with a numerical method (Galerkin, least squares method, etc.).

4.5.2. The application to the second example

As another application, consider the following modified equation again from [52],

$$\ddot{u} + {\omega_0}^2 u = -\varepsilon (D^\alpha u)^3 \tag{81}$$

Thus,

$$\begin{aligned} f(u_0, {D_0}^2 u_0, D^\alpha u_0) &= -(D^\alpha u_0)^3 \\ &= -\omega_0^{3\alpha} a^3 \cos^3\left(\phi + \frac{\pi\alpha}{2}\right) \end{aligned} \tag{82}$$

For this f, inserting (81) into (22) and (23), the following equations are obtained

$$\begin{aligned} a' &= -\frac{1}{2\pi\omega_0}\int_0^{2\pi} \sin\phi \left(-\omega_0^{3\alpha} a^3 \cos^3\left(\phi + \frac{\pi\alpha}{2}\right)\right) d\phi \\ &= -\frac{3a^3 {\omega_0}^{3\alpha-1}}{8} \sin\left(\frac{\pi\alpha}{2}\right) \end{aligned} \tag{83}$$

$$\begin{aligned} \beta' &= -\frac{1}{2\pi\omega_0 a}\int_0^{2\pi} \cos\phi \left(-\omega_0^{3\alpha} a^3 \cos^3\left(\phi + \frac{\pi\alpha}{2}\right)\right) d\phi \\ &= \frac{3a^2 {\omega_0}^{3\alpha-1}}{8} \cos\left(\frac{\pi\alpha}{2}\right). \end{aligned} \tag{84}$$

Integrating (83) and (84) yields,

$$a = \pm \frac{2}{\sqrt{3{\omega_0}^{3\alpha-1} \sin\left(\frac{\pi\alpha}{2}\right)\varepsilon t + 4a_0}} \tag{85}$$

and

$$\beta = \frac{1}{2}\cot\left(\frac{\pi\alpha}{2}\right) \ln\left(6\varepsilon t {\omega_0}^{3\alpha} \sin\left(\frac{\pi\alpha}{2}\right) + 8a_0\omega_0\right) + \beta_0 \tag{86}$$

where a_0 and β_0 are constants. Consequently, (24) is obtained with a and β, which are given by (85) and (86), respectively. Therefore, (24) becomes

$$u = \pm \frac{2\cos\left(\omega t + \frac{1}{2}\cot\left(\frac{\pi\alpha}{2}\right)\ln\left(6\varepsilon t {\omega_0}^{3\alpha}\sin\left(\frac{\pi\alpha}{2}\right) + 8a_0\omega_0\right) + \beta_0\right)}{\sqrt{3{\omega_0}^{3\alpha-1}\sin\left(\frac{\pi\alpha}{2}\right)\varepsilon t + 4a_0}} + O(\varepsilon). \tag{87}$$

In Fig. 12, the exact solution of (81), the variation of the amplitude and phase according to α are plotted. As α increases, the nonlinear

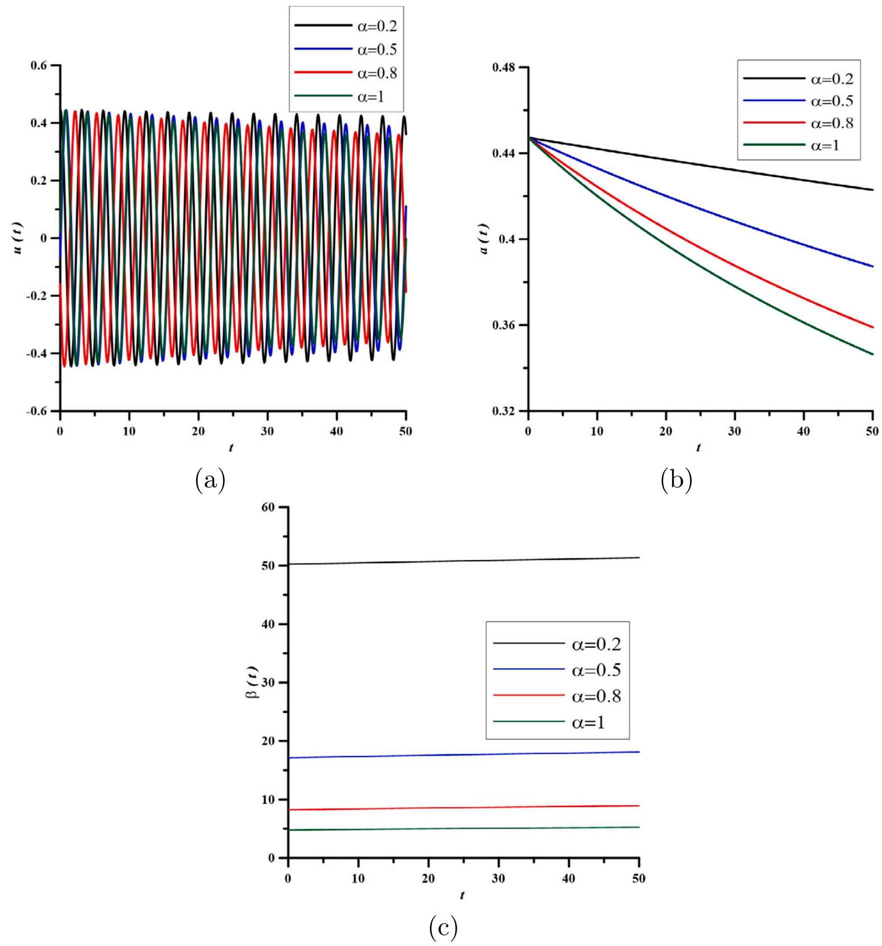

Fig. 11. (a) The solution function $u(t)$, (b) the amplitude $a(t)$ and (c) the phase $\beta(t)$ of (74) for $\varepsilon = 1/3$, $a_0 = 5$, $\omega_0 = 2$, $\beta_0 = 0$.

fractional term acts as a damping; also, like 4.5.1, the rate of amplitude change increases in a curvilinear manner, while the rate of phase change remains approximately constant. For $\alpha = 1$, β remains constant and there is no stiffness effect. In addition, to compare, non-fractional graphs for the equation are displayed in Fig. 12.

5. Comparison

This section presents a validation of the proposed general model by examining its consistency with the existing solutions of oscillators in the literature. The model is evaluated by comparing it with existing solutions, which are numerically verified in the literature for well-known nonlinear oscillators, specifically the fractional Duffing and the fractional Van der Pol oscillators. Furthermore, comparative analyses are conducted across different damped models, including classical and fractional approaches, to illustrate the impact of damping types on vibration amplitude reduction.

A special case of the considered Duffing oscillator with fractional-order derivative in Ref. [54] (see Eq. (3), page 3093) is considered in Application 4.1.1, where the fractional Duffing oscillator excludes both external excitation and linear viscous damping. The parameters in the referenced study correspond to the following parameters in this paper: $x = u,\ \mu = 0,\ \alpha = 1,\ k_1 = 2\mu,\ p = \alpha,\ f = 0,\ \sigma = 0$. (The left-hand sides are the parameters in the referenced paper, and the right-hand sides are the parameters in this paper.) Taking these correspondences into account, the solutions of the system Eqs. (20a)–(20b) in [54] and the solutions of the system Eqs. (31)–(32) are identical. Note that, since the multiple time scales is used in this paper, $T_1 = \varepsilon t$. This also demonstrates clear consistency between the proposed general model and the referenced solution. Additionally, note that, as the abovementioned reasons in Section 2, using either the definition of Riemann–Liouville or the definition of the Caputo does not make any difference. In summary, the obtained results demonstrate consistency between the referenced solution in Ref. [54], thus confirming the convenience of the proposed general model.

In addition, Application 4.4.1, the fractional Van der Pol oscillator (Eq. (67)), is a special case of the model in the Ref. [53]. In the referenced article, the Van der Pol oscillator with two kinds of fractional-order derivatives is considered, whereas this study considers the Van der Pol oscillator with a single kind of fractional-order derivative. That is, the fractional Van der Pol Eq. (67), modeled using only the fractional parameter α within the range of 0 to 1, is considered. Considering correspondences, the solutions of the system Eqs. (10)–(11) from [53] and the solutions of the system Eqs. (69)–(70) are identical. Note that, as the method of multiple time scales is employed in this paper, $T_1 = \varepsilon t$. This also demonstrates a consistency between the proposed general model and the referenced solution.

As seen in Figs. 1–5, 9–12, validation has been performed by comparing classical damped models, which correspond to $\alpha = 1$, with each damped model. The solutions obtained are the same as the classical solutions presented in [1]. Thus, the consistency of the obtained results with the literature has been demonstrated. So, it has been proven that the use of the Riemann–Liouville derivative is suitable for dynamic problems.

Additionally, damped models have been compared among themselves. Fig. 13 shows a comparison of different damped models. While obtaining these graphs, initial boundary conditions were chosen so that the arbitrary constants in the solution were the same for each model.

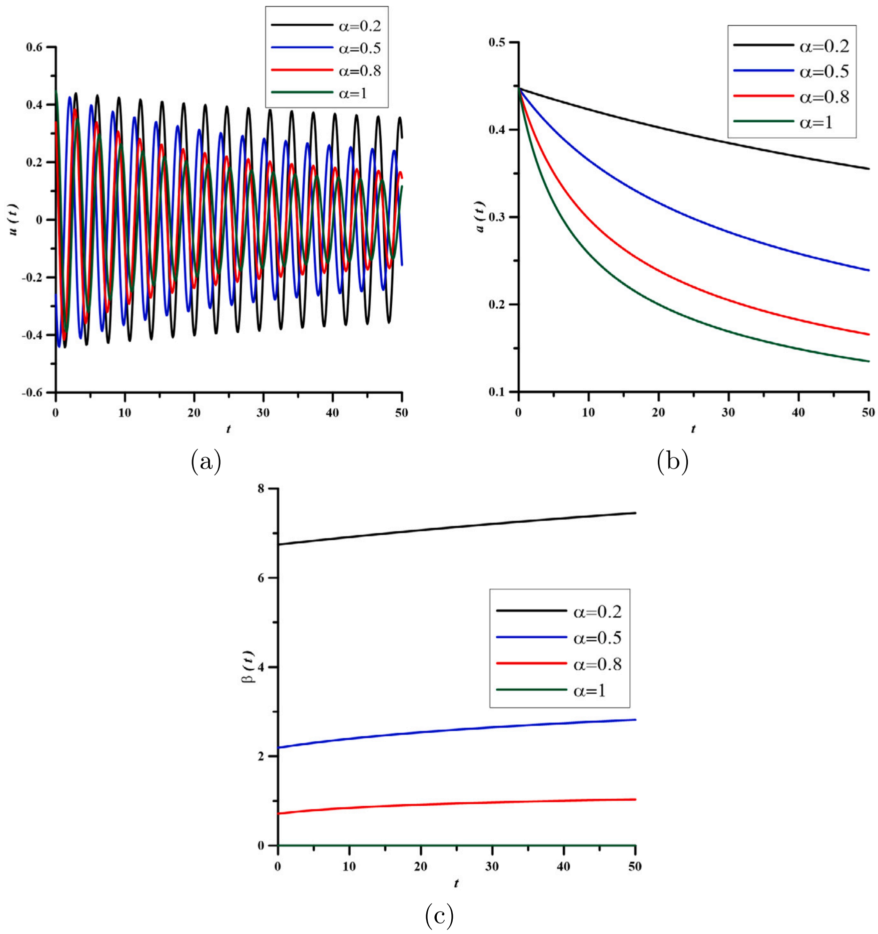

Fig. 12. (a) the solution function $u(t)$, (b) the amplitude $a(t)$ and (c) the phase $\beta(t)$ of (81) for $\varepsilon = 1/3$, $a_0 = 5$, $\omega_0 = 2$, $\beta_0 = 0$.

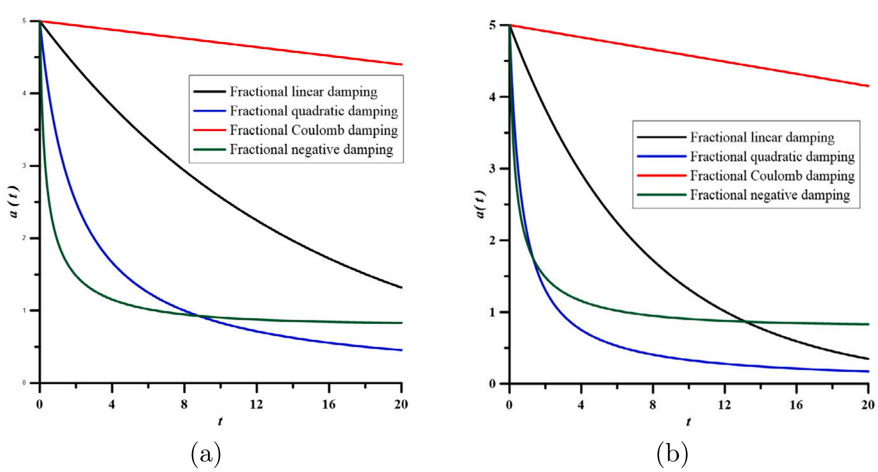

Fig. 13. Comparison of amplitude variation for $\varepsilon = 1/3$, $a_0 = 5$, $\mu = 0.4$, $\omega_0 = 2$, $\beta_0 = 0$. (a) fractionally damped models for $\alpha = 0.5$ (b) conventional models, i.e. $\alpha = 1$.

As a result of this comparison, the most effective damped model is the quadratic damped model. On the other hand, the damped model with the smallest reduction in vibration amplitude is the Coulomb-type damping. This information is important for vibration control. These results obtained for fractionally damped models are also valid for conventional models.

6. Concluding remarks

This study presents a general solution procedure that is suitable for various fractionally damped mechanisms, linear and nonlinear fractional equations. The method of multiple time scales is directly implemented to calculate the semi-analytical solutions. In the solution procedure, Fourier series are employed in the expansion of the ordered term.

The main results can be summarized as follows:

- A novel general model, not previously found in the literature, has been proposed.
- It has been demonstrated that the solution with the Fourier series is also suitable for the fractional models.
- The obtained results allow us to analyze the effects of various types of damping on the behaviors of systems having a single-degree-of-freedom.
- Additionally, the proposed procedure is applied to the fractional nonlinear equations involving nonlinear terms, which consists of acceleration or displacement.
- For $\alpha = 1$, the obtained solutions coincide with the non-fractional models given in the literature.
- For the negative damped case, while the initial amplitude is less than the steady amplitude value, i.e., $a_0 < a_s$ the damping effect decreases as α increases. In contrast, the opposite is true for the other cases, i.e., the damping effect increases as α increases.
- The most effective damped model is the quadratic damped model.
- The damped model with the smallest reduction in vibration amplitude is the Coulomb-type damping.
- The comparison conclusions for fractionally damped models are also valid for conventional models.
- A comparative analysis is conducted with an existing solution from the literature that is numerically verified and accepted to validate the accuracy and reliability of the proposed general model. The results demonstrate consistency between the solution of the proposed general model and the referenced solution, confirming the correctness of the general model results.

The discovery of a general solution not only streamlines analysis and computation but also catalyzes further research and innovation in the field. Researchers can focus on refining the model, validating it against experimental data, and exploring practical applications in real-world engineering scenarios.

CRediT authorship contribution statement

Bengi Yıldız: Writing – review & editing, Writing – original draft, Visualization, Validation, Methodology, Investigation, Formal analysis, Data curation, Conceptualization. **Sümeyye Sınır:** Writing – review & editing, Writing – original draft, Visualization, Validation, Methodology, Investigation, Formal analysis, Data curation, Conceptualization. **Berra Gültekin Sınır:** Writing – review & editing, Visualization, Validation, Supervision, Methodology, Investigation, Formal analysis, Data curation, Conceptualization.

Declaration of competing interest

The authors declare that they have no known competing financial interests or personal relationships that could have appeared to influence the work reported in this paper.

The author is an Editorial Board Member/Editor-in-Chief/Associate Editor/Guest Editor and was not involved in the editorial review or the decision to publish this article.

Data availability

No data was used for the research described in the article.

References

[1] A.H. Nayfeh, D.T. Mook, Nonlinear Oscillations, John Wiley & Sons, 2008.
[2] G.D. Hatzigeorgiou, D.E. Beskos, Inelastic displacement ratios for SDOF structures subjected to repeated earthquakes, Eng. Struct. 31 (11) (2009) 2744–2755.
[3] C. Christopoulos, A. Filiatrault, B. Folz, Seismic response of self-centring hysteretic SDOF systems, Earthq. Eng. Struct. Dyn. 31 (5) (2002) 1131–1150.
[4] P. Andreas, K. Moris, A. Ioannis, F. Lina, Acoustic performance evaluation of a panel utilizing negative stiffness mounting for low frequency noise control, in: Proc Int Conf Struct Dyn, EURODYN, Vol. 2, 2020, pp. 4093–4110.
[5] A.A. Nikooyan, A.A. Zadpoor, Mass–spring–damper modelling of the human body to study running and hopping–an overview, Proc. Inst. Mech. Eng. H 225 (12) (2011) 1121–1135.
[6] S. Sınır, B. Yıldız, B.G. Sınır, Approximate solutions of nonlinear pendulum with fractional damping, in: 5th International Students Science Congress Proceedings Book, 2021, p. 295.
[7] Z. Huang, X. Jin, Response and stability of a SDOF strongly nonlinear stochastic system with light damping modeled by a fractional derivative, J. Sound Vib. 319 (3–5) (2009) 1121–1135.
[8] W. Staszewski, Identification of damping in MDOF systems using time-scale decomposition, J. Sound Vib. 203 (2) (1997) 283–305.
[9] J. Wang, Y. Shen, S. Yang, Y. Lu, X. Li, D. Zuo, Dynamic response of a piecewise linear single-degree-of-freedom oscillator with fractional-order derivative, J. Low Freq. Noise Vib. Act. Control 40 (1) (2021) 72–83.
[10] J. Yuan, Y. Zhang, J. Liu, B. Shi, M. Gai, S. Yang, Mechanical energy and equivalent differential equations of motion for single-degree-of-freedom fractional oscillators, J. Sound Vib. 397 (2017) 192–203.
[11] O. Zarraga, I. Sarría, J. García-Barruetabeña, F. Cortés, An analysis of the dynamical behaviour of systems with fractional damping for mechanical engineering applications, Symmetry 11 (12) (2019) 1499.
[12] Z. Wang, H. Hu, Stability of a linear oscillator with damping force of the fractional-order derivative, Sci. China Phys. Mech. Astron. 53 (2010) 345–352.
[13] A. Shokooh, L. Suárez, A comparison of numerical methods applied to a fractional model of damping materials, J. Vib. Control 5 (3) (1999) 331–354.
[14] Y.A. Rossikhin, M. Shitikova, Analysis of nonlinear vibrations of a two-degree-of-freedom mechanical system with damping modelled by a fractional derivative, J. Eng. Math. 37 (4) (2000) 343–362.
[15] J. Jiang, D. Cao, H. Chen, K. Zhao, The vibration transmissibility of a single degree of freedom oscillator with nonlinear fractional order damping, Int. J. Syst. Sci. 48 (11) (2017) 2379–2393.
[16] J. Wang, R. Zhang, J. Liu, Vibrational resonance analysis in a fractional order Toda oscillator model with asymmetric potential, Int. J. Non-Linear Mech. 148 (2023) 104258.
[17] I. Podlubny, Fractional differential equations, in: vol. 198 of Mathematics in Science and Engineering, 1999.
[18] K.S. Miller, B. Ross, An Introduction to the Fractional Calculus and Fractional Differential Equations, Wiley, 1993.
[19] L. Debnath, Recent applications of fractional calculus to science and engineering, Int. J. Math. Math. Sci. 2003 (54) (2003) 3413–3442.
[20] M. Javadi, M. Noorian, S. Irani, Stability analysis of pipes conveying fluid with fractional viscoelastic model, Meccanica 54 (2019) 399–410.
[21] R. Lewandowski, P. Wielentejczyk, Nonlinear vibration of viscoelastic beams described using fractional order derivatives, J. Sound Vib. 399 (2017) 228–243.
[22] D. Dönmez Demir, N. Bildik, B. Sınır, Linear dynamical analysis of fractionally damped beams and rods, J. Engrg. Math. 85 (2014) 131–147.
[23] Y. Tang, Y. Zhen, B. Fang, Nonlinear vibration analysis of a fractional dynamic model for the viscoelastic pipe conveying fluid, Appl. Math. Model. 56 (2018) 123–136.
[24] X. Yang, Z. Sun, Research on parametric resonance in a stochastic van der pol oscillator under multiple time delayed feedback control, Int. J. Non-Linear Mech. 45 (6) (2010) 621–627.
[25] P. Balasubramanian, G. Ferrari, M. Amabili, Identification of the viscoelastic response and nonlinear damping of a rubber plate in nonlinear vibration regime, Mech. Syst. Signal Process. 111 (2018) 376–398.
[26] M. Amabili, Derivation of nonlinear damping from viscoelasticity in case of nonlinear vibrations, Nonlinear Dynam. 97 (3) (2019) 1785–1797.
[27] M. Amabili, Nonlinear damping in large-amplitude vibrations: modelling and experiments, Nonlinear Dynam. 93 (1) (2018) 5–18.
[28] M. Amabili, Nonlinear damping in nonlinear vibrations of rectangular plates: derivation from viscoelasticity and experimental validation, J. Mech. Phys. Solids 118 (2018) 275–292.
[29] F. Alijani, M. Amabili, P. Balasubramanian, S. Carra, G. Ferrari, R. Garziera, Damping for large-amplitude vibrations of plates and curved panels, part 1: Modeling and experiments, Int. J. Non-Linear Mech. 85 (2016) 23–40.
[30] S. Zaitsev, O. Shtempluck, E. Buks, O. Gottlieb, Nonlinear damping in a micromechanical oscillator, Nonlinear Dynam. 67 (2012) 859–883.
[31] B. Karthik, R.B. Shreesha, V. Shrikanth, A.K. Gaonkar, Prediction of energy dissipation by analytical solution to combined viscous and Coulomb damping, J. Sound Vib. 573 (2024) 118216.
[32] N. Mostaghel, T. Davis, Representations of Coulomb friction for dynamic analysis, Earthq. Eng. Struct. Dyn. 26 (5) (1997) 541–548.

[33] O. Gottlieb, G. Habib, Non-linear model-based estimation of quadratic and cubic damping mechanisms governing the dynamics of a chaotic spherical pendulum, J. Vib. Control 18 (4) (2012) 536–547.

[34] A.H. Salas, S. El-Tantawy, N.H. Aljahdaly, An exact solution to the quadratic damping strong nonlinearity duffing oscillator, Math. Probl. Eng. 2021 (1) (2021) 8875589.

[35] R. Fangnon, C. Ainamon, A.V. Monwanou, C. Miwadinou, J. Chabi Orou, Nonlinear dynamics of the quadratic-damping Helmholtz oscillator, Complexity 2020 (1) (2020) 8822534.

[36] M. Amabili, P. Balasubramanian, G. Ferrari, Nonlinear vibrations and damping of fractional viscoelastic rectangular plates, Nonlinear Dynam. 103 (2021) 3581–3609.

[37] D. Dönmez Demir, N. Bildik, B.G. Sinir, Linear vibrations of continuum with fractional derivatives, Bound. Value Probl. 2013 (2013) 1–15.

[38] B.G. Sınır, Infinite mode analysis of a general model with external harmonic excitation, Appl. Math. Model. 39 (7) (2015) 1823–1836.

[39] B.B. Özhan, M. Pakdemirli, A general solution procedure for the forced vibrations of a continuous system with cubic nonlinearities: primary resonance case, J. Sound Vib. 325 (4–5) (2009) 894–906.

[40] M.H. Ghayesh, S. Kazemirad, M.A. Darabi, A general solution procedure for vibrations of systems with cubic nonlinearities and nonlinear/time-dependent internal boundary conditions, J. Sound Vib. 330 (22) (2011) 5382–5400.

[41] W. Lacarbonara, Direct treatment and discretizations of non-linear spatially continuous systems, J. Sound Vib. 221 (5) (1999) 849–866.

[42] M. Pakdemirli, M. Karahan, H. Boyacı, A new perturbation algorithm with better convergence properties: Multiple scales Lindstedt Poincaré method, Math. Comput. Appl. 14 (1) (2009) 31–44.

[43] M. Pakdemirli, M.M.F. Karahan, A new perturbation solution for systems with strong quadratic and cubic nonlinearities, Math. Methods Appl. Sci. 33 (6) (2010) 704–712.

[44] Y.A. Rossikhin, M.V. Shitikova, On fallacies in the decision between the Caputo and Riemann–Liouville fractional derivatives for the analysis of the dynamic response of a nonlinear viscoelastic oscillator, Mech. Res. Commun. 45 (2012) 22–27.

[45] B.G. Sınır, Comments on ‘‘asymptotic analysis of an axially viscoelastic string constituted by a fractional differentiation law’’, Int. J. Non-Linear Mech. 59 (2014) 83–84.

[46] A.A. Kilbas, O.I. Marichev, S.G. Samko, Fractional integrals and derivatives (theory and applications), 1993.

[47] Y.A. Rossikhin, M. Shitikova, Application of fractional derivatives for the analysis of nonlinear damped vibrations of suspension bridges, in: Proceedings 1997 International Symposium on Nonlinear Theory and Its Applications. NOLTA'97, 1997, pp. 541–544.

[48] Y.A. Rossikhin, M.V. Shitikova, New approach for the analysis of damped vibrations of fractional oscillators, Shock Vib. 16 (4) (2009) 365–387.

[49] Y.A. Rossikhin, M.V. Shitikova, Application of fractional calculus for dynamic problems of solid mechanics: novel trends and recent results, 2010.

[50] D. Dönmez Demir, N. Bildik, B. Sinir, Application of fractional calculus in the dynamics of beams, Bound. Value Probl. 2012 (1) (2012) 1–13.

[51] Y. Shen, S. Yang, H. Xing, H. Ma, Primary resonance of duffing oscillator with two kinds of fractional-order derivatives, Int. J. Non-Linear Mech. 47 (9) (2012) 975–983.

[52] A.H. Nayfeh, Introduction to Perturbation Techniques, John Wiley & Sons, 2011.

[53] Y. Shen, S. Yang, C. Sui, Analysis on limit cycle of fractional-order van der pol oscillator, Chaos Solitons Fractals 67 (2014) 94–102.

[54] Y. Shen, S. Yang, H. Xing, G. Gao, Primary resonance of duffing oscillator with fractional-order derivative, Commun. Nonlinear Sci. Numer. Simul. 17 (7) (2012) 3092–3100.